RESEARCH PAPER

FORMULATION, OPTIMIZATION AND EVALUATION OF MICONAZOLE NITRATE NANOCRYSTAL-LOADED TOPICAL GEL WITH GLYCOLIC ACID FOR ENHANCED ANTIFUNGAL DELIVERY

Short Title: Miconazole Nitrate Nanocrystal Gel with Glycolic Acid

Sheela Yadav, Priyanka Goswami*, Jaya Agnihotri, Mohammad Wais, Saima Shaikh
H. K. College of Pharmacy, Oshiwara, Jogeshwari (West), Mumbai – 400102, Maharashtra, India
*Corresponding author. E-mail: priyanka8408@gmail.com

ABSTRACT
Miconazole nitrate is a widely used topical azole antifungal whose clinical performance is limited by poor aqueous solubility, which restricts its dissolution and penetration across the stratum corneum. This study aimed to formulate and evaluate a miconazole nitrate nanocrystal (MNNC)-loaded topical gel, combined with glycolic acid, to improve dermal delivery and antifungal efficacy against *Candida albicans*. Nanocrystals were prepared by nanoprecipitation using poloxamer 407 as a steric stabilizer, and the process was optimized using a three-factor, three-level Box–Behnken design with poloxamer 407 concentration, sonication time and homogenization speed as independent variables, and percentage yield and particle size as responses. A UV spectrophotometric method was developed and validated for quantification of miconazole nitrate, showing linearity over 2–10 µg/mL ($r = 0.9991$) with acceptable precision and accuracy. The optimized nanocrystal batch (1.00% w/v poloxamer 407, 17.58 min sonication, 2423 rpm homogenization) yielded particles of 256.5 nm with 72.76% yield. Nanocrystals were characterized by FTIR, SEM, optical microscopy, PXRD and DSC, confirming excipient compatibility and retention of crystallinity. MNNC was incorporated into a Carbopol 934 gel base; the optimized gel (composition H3) showed a viscosity of 2112 cP, pH 5.5, spreadability of 34.41 g·cm/s, extrudability of 88.19% and 86.5% cumulative *in vitro* drug release over 7 hours, outperforming a marketed miconazole gel (53.9% release). *Ex vivo* permeation through excised goat skin gave 48.03% cumulative permeation over 8 hours, with drug preferentially retained in the epidermis. The formulated gel produced a larger zone of inhibition against *C. albicans* than the marketed product and remained stable over 3 months under ICH-recommended long-term and accelerated conditions. These findings indicate that an MNNC-loaded gel combined with glycolic acid as a penetration enhancer is a promising strategy to improve the topical antifungal performance of a poorly water-soluble drug.

Keywords: Miconazole nitrate; Nanocrystals; Box–Behnken design; Glycolic acid; Topical gel; *Candida albicans*; *Ex vivo* permeation.

How to cite this article: Sheela Yadav Priyanka Goswami* Jaya Agnihotri Mohammad Wais Saima Shaikh. FORMULATION, OPTIMIZATION AND EVALUATION OF MICONAZOLE NITRATE NANOCRYSTAL-LOADED TOPICAL GEL WITH GLYCOLIC ACID FOR ENHANCED ANTIFUNGAL DELIVERY. Int J Drug Deliv Technol. 2026;16(80s):1318-1330. DOI: 10.25258/ijddt.16.80s.167

.INTRODUCTION

Poor aqueous solubility remains one of the most significant challenges in modern drug development, with a large proportion of new chemical entities falling into Class II or IV of the Biopharmaceutics Classification System, in which dissolution rather than permeability limits absorption.[1] Conventional approaches to overcome this limitation, including salt formation, cosolvency, complexation and micronization, are often inadequate for drugs with very low solubility, prompting a shift from micronization to nanonization. Drug nanocrystals — pure, carrier-free solid particles with a mean diameter below 1 µm — represent a versatile nanonization strategy that increases the effective surface area of a drug, thereby enhancing its saturation solubility, dissolution velocity and adhesiveness to biological surfaces; adequate steric or electrostatic stabilization of the newly created surface is the principal formulation challenge.[2,3] The topical route is particularly well suited to such carriers, since drug can be concentrated at the site of action while systemic exposure is minimised.[4] Nanosized carriers additionally act as permeation enhancers in their own right, promoting deposition within the stratum corneum and follicular openings, and a wide range of such systems has reached dermatological and dermo-cosmetic products.[5,6]

Superficial fungal infections affect a substantial proportion of the global population and are caused predominantly by dermatophytes and yeasts such as *Candida albicans*.[7,8] Miconazole nitrate, an imidazole-derivative antifungal, acts by inhibiting fungal cytochrome P450-dependent 14α-demethylase, thereby blocking ergosterol biosynthesis and compromising membrane integrity, and is widely used topically for such infections.[9] Its clinical effectiveness is nevertheless constrained by low aqueous solubility, which limits dissolution at the site of application and consequently reduces penetration through the stratum corneum. A wide range of nanocarriers has therefore been investigated

for miconazole nitrate, including solid lipid nanoparticles,[10] lipid-based nanocarriers,[11] natural-polymer nanoparticulate systems,[12] transethosomes,[13] nanosuspensions stabilized with cellulose ethers or poloxamers,[14,15] dermal nanocrystals,[16] nanocrystal-loaded hydrogels[17] and polymeric or lipid nanocapsules.[18] Comparable nanocrystal and fibre-based approaches have been reported for luliconazole,[19,20] and lipid-nanoparticle gels have been used for fluconazole[21] and for non-antifungal topical actives.[22]

Formulating miconazole nitrate as nanocrystals offers a carrier-free means of improving its dissolution rate and, in turn, its skin permeation and retention, without requiring large quantities of excipients. Previous dermal nanocrystal work has shown that the benefit of the nanocrystalline state can be amplified by including a second, mechanistically complementary agent in the vehicle.[16] In the present work, glycolic acid, an alpha-hydroxy acid, was selected for this role. Glycolic acid acts as a chemical penetration enhancer by disrupting the ordered lipid structure of the stratum corneum, and independently exerts keratolytic and exfoliative activity that reduces corneocyte cohesion and removes dead, infected keratinized tissue, thereby helping to interrupt fungal growth.[23] The combination of nanocrystal technology with a penetration-enhancing, keratolytic co-agent was therefore hypothesised to produce a synergistic improvement in topical antifungal therapy. To the best of our knowledge, the use of free glycolic acid as a combined penetration enhancer and keratolytic within an antifungal nanocrystal gel has not previously been reported.

The present study describes the nanoprecipitation-based preparation of miconazole nitrate nanocrystals (MNNC), their optimization using a Box–Behnken statistical design, their incorporation into a Carbopol 934 gel base together with glycolic acid, and a comprehensive evaluation of the resulting formulation — including physicochemical characterization, *in vitro* release, *ex vivo* skin permeation and retention, *in vitro* antifungal activity against *C. albicans* and short-term stability — benchmarked against a marketed miconazole gel.

MATERIALS AND METHODS

Materials

Miconazole nitrate was received as a gift sample from Maharshee Laboratories Pvt. Ltd. (Ankleshwar, Gujarat, India). Glycolic acid, polyethylene glycol (PEG), propylene glycol, poloxamer 407, methanol, ethanol, Carbopol 940 and Carbopol 934 were procured from Ozone International (Mumbai, India). Oleic acid, glycerin, disodium edetate (EDTA) and triethanolamine were procured from Chemdyes Corporation (Ahmedabad, India), and methyl paraben, propyl paraben and sodium benzoate from S. D. Fine Chemicals (Mumbai, India). HPMC K-100, polyvinylpyrrolidone (PVP) and nutrient agar were obtained from Vishal Chem (Mumbai, India). *Candida albicans* (MTCC 183) was procured from the Microbial Type Culture Collection, Chandigarh, India. Distilled water was used throughout, and all chemicals were of analytical grade.

Preformulation studies

Aqueous solubility of miconazole nitrate was determined by the saturation shake-flask method: an excess of drug was dispersed in distilled water and in phosphate-buffered saline (pH 5.5), shaken at 50 rpm and 37 °C for 72 h, filtered and analysed by UV spectroscopy at 272 nm. Lipophilicity (log P) was determined by the shake-flask method using *n*-octanol and acetate buffer (pH 5.5), agitated for 72 h to reach equilibrium, with drug quantified in each phase by UV spectroscopy. Drug–excipient compatibility was assessed by holding 1:1 mixtures of miconazole nitrate with each excipient (Carbopol 934, oleic acid, glycerin, propyl paraben, methyl paraben, sodium benzoate, HPMC K-100, triethanolamine, PEG, glycolic acid and PVP) at 25 °C/75% RH and 40 °C/75% RH, with visual and FTIR monitoring at 0, 7, 15 and 30 days.

UV spectrophotometric method development and validation

A UV method for miconazole nitrate estimation was developed and validated on a Shimadzu UV-1800 double-beam spectrophotometer (Shimadzu Corporation, Kyoto, Japan), scanning between 200 and 400 nm to determine λmax. A standard stock solution was prepared by dissolving 10 mg of miconazole nitrate in methanol and diluting to volume; working solutions of 2–10 µg/mL were prepared by serial dilution. The method was validated in accordance with ICH Q2(R1)[24] for linearity, precision (intraday and interday), accuracy (recovery by standard addition at 80%, 100% and 120% of the target concentration, in triplicate), and limit of detection (LOD) and limit of quantification (LOQ), calculated as $3.3\sigma/S$ and $10\sigma/S$ respectively, where σ is the residual standard deviation of the regression line and S is the slope of the calibration curve.

Preparation of miconazole nitrate nanocrystals

MNNC were prepared by nanoprecipitation (solvent–antisolvent precipitation), in which rapid diffusion of a water-miscible organic solvent into an aqueous antisolvent generates local supersaturation and instantaneous nucleation of submicron particles.[25] Poloxamer 407 (0.75–1.25% w/v) was used as the dispersion stabilizer. Briefly, 10 mL of organic phase (0.05% w/v miconazole nitrate in methanol) was injected into 50 mL of aqueous poloxamer 407 solution through a 22-gauge syringe under continuous mechanical stirring at 2000 rpm, with the aqueous phase maintained at 2 °C in an ice bath to promote instantaneous precipitation and prevent uncontrolled crystal growth. The resulting dispersion was stirred for a further 30 min and then

probe-sonicated (20 kHz, 1500 W) for a variable duration at 25 °C. Nanocrystals were harvested by cooling centrifugation (10,000 rpm, 4 °C, 10 min), re-dispersed in distilled water, filtered through a 0.2 µm Whatman membrane and air-dried at room temperature.

Experimental design and optimization

Preliminary trials identified poloxamer 407 concentration, sonication time and homogenization speed as the process variables with the greatest influence on particle size and yield. These were optimized using a three-factor, three-level Box–Behnken design[26] (Design-Expert® software version 13; Stat-Ease Inc., Minneapolis, MN, USA), generating 15 experimental runs including three centre points. Percentage yield (Y1) and particle size (Y2) were selected as dependent responses and fitted to a second-order polynomial model:

$$R = b0 + b1A + b2B + b3C + b12AB + b13AC + b23BC + b11A^2 + b22B^2 + b33C^2$$

where R is the response, b0 the intercept, b1–b33 the regression coefficients, and A, B and C represent poloxamer 407 concentration, sonication time and homogenization speed respectively. The independent variables and their coded levels are shown in Table 1.

Table 1: Independent variables and their levels used in the Box–Behnken design

Factor	Low (–1)	Medium (0)	High (+1)
Poloxamer 407 concentration (% w/v)	0.75	1.00	1.25
Sonication time (min)	10	17.5	25
Homogenization speed (rpm)	1000	3000	5000

Characterization of nanocrystals

Particle size (Z-average) was measured by dynamic light scattering. Drug content was determined by dissolving 5 mg of nanocrystals in ethanol, filtering and assaying by UV spectroscopy at 272 nm. Morphology was examined by scanning electron microscopy (SEM) and optical microscopy. Crystallinity was assessed by powder X-ray diffraction (PXRD; D8 Advance diffractometer, Bruker, Karlsruhe, Germany; 2θ range 5–40°) and differential scanning calorimetry (DSC; EXSTAR TG/DTA 6300, Seiko Instruments, Chiba, Japan; 10 °C/min, nitrogen atmosphere). Drug–excipient interactions were investigated by FTIR (Shimadzu IRAffinity-1S; KBr pellet method, 4000–400 cm^{-1}). *In vitro* dissolution of the nanocrystals was evaluated using USP Apparatus 2 in 900 mL of pH 5.5 acetate buffer (50 rpm, 37 ± 0.5 °C) over 8 h, with samples withdrawn at fixed intervals and assayed at 272 nm. Short-term stability of the nanosuspension was assessed at room temperature, 2 °C and 40 °C over 7 days, monitoring particle size.

Preparation of nanocrystal-loaded topical gel

Placebo gel bases were first screened using HPMC K-100 over four batches (B1–B4) at 0.25–1% w/v, with EDTA, glycerin, propylene glycol and propyl paraben held constant and triethanolamine used to adjust pH (Table 2). Viscosity increased with HPMC K-100 concentration and 1% w/v gave the best gel-forming behaviour; however, on addition of glycolic acid the acidic medium depolymerized HPMC K-100, causing an unacceptable loss of viscosity, and this polymer was therefore excluded.

Carbopol 934 was selected as the gelling agent for the final formulation on the basis of its established pseudoplastic, thixotropic behaviour and rheological stability across the dermatological pH range,[27] its ability to deliver a viscosity of 2000–5000 cP appropriate for topical application, and the successful use of semisolid vehicles of this type for azole antifungals.[28] Preservatives (methyl and propyl paraben) were dispersed in the penetration enhancer with gentle stirring (100 rpm) and heating (50 °C). Carbopol 934 was dispersed slowly into water and allowed to hydrate for 24 h, followed by stirring at 600 rpm for 30 min and addition of humectant. The optimized MNNC dispersion was vortexed for 15 min and incorporated into the polymeric dispersion under vigorous stirring (1200 rpm, 15 min). Glycolic acid was added as the penetration enhancer, and the pH was adjusted dropwise with triethanolamine until a clear, homogeneous, viscous gel was obtained. Five batches (H1–H5) were prepared in which the Carbopol 934 concentration was increased stepwise while the quantities of all other components were held constant.

Table 2: Composition of the placebo gel bases screened with HPMC K-100 (batches B1–B4)

Ingredient	B1	B2	B3	B4
HPMC K-100	0.25 g	0.50 g	0.75 g	1.00 g
Glycerin	0.50 g	1.00 g	1.00 g	1.00 g

Ingredient	B1	B2	B3	B4
Propylene glycol	0.50 g	0.50 g	0.25 g	0.25 g
EDTA	10 mg	10 mg	10 mg	10 mg
Propyl paraben	0.05 % w/v	0.05 % w/v	0.05 % w/v	0.05 % w/v
Triethanolamine	2 drops	2 drops	2 drops	2 drops
Distilled water	q.s.	q.s.	q.s.	q.s.

Evaluation of topical gel

Viscosity was measured using a Brookfield DV-E viscometer (spindle 64, 12 rpm) on 10 g of gel. Drug content uniformity was assessed by extracting and assaying the top, middle and bottom layers of the gel at 272 nm. pH was measured using a Systronics digital pH meter. Spreadability (S, g·cm/s) was determined by the glass-slide method and calculated as $S = m \times L / t$, where m is the weight of the load (g), L is the distance travelled by the upper slide (cm) and t is the time taken (s). Extrudability was assessed from the percentage of gel extruded from a sealed collapsible aluminium tube under standard pressure. *In vitro* drug release from the gel batches was evaluated using USP Apparatus 2 in 900 mL of pH 5.5 acetate buffer (50 rpm, 37 ± 0.5 °C), with samples withdrawn at fixed intervals and assayed at 272 nm; a marketed miconazole nitrate gel (Miconit) was tested in parallel as reference.

***Ex vivo* permeation and skin retention study**

Ex vivo permeation was studied in a Franz diffusion cell in accordance with the principles of OECD Test Guideline 428 for *in vitro* skin absorption,[29] using excised goat skin with the stratum corneum facing the donor compartment. Goat skin was selected as the membrane because it is readily available as an abattoir by-product and has been used and characterised alongside other animal skins in comparative *ex vivo* permeation studies of topical gels.[30] Skin was cleaned, defatted and examined for integrity before mounting. The receptor compartment contained 20 mL of phosphate buffer (pH 7.4), stirred at 100 rpm and maintained at 37 ± 0.5 °C. Two grams of gel were applied to the donor compartment, and samples were withdrawn hourly for 8 h with immediate replacement of an equal volume of fresh medium, and analysed by UV spectroscopy at 272 nm. At the end of the study, the stratum corneum, epidermis and dermis were separated by careful dissection, and drug retained within each layer was extracted in methanol, sonicated, centrifuged, filtered and assayed. Drug retained in each layer is expressed as a percentage of the total drug recovered from the skin.

***In vitro* antifungal activity**

C. albicans (MTCC 183) was maintained on Sabouraud dextrose agar slants incubated at 37 °C. Antifungal activity was assessed by the agar well diffusion (cup-plate) method on nutrient agar plates seeded with an overnight culture of the organism. Wells were cut using a sterile borer and loaded with the nanocrystal-incorporated gel and the marketed miconazole nitrate gel at equivalent drug loading, together with a control well. Plates were incubated for 24 h and the zone of inhibition was measured. Determinations were performed in triplicate.

Stability studies

Stability of the nanocrystal suspension and the finished gel was assessed as per ICH Q1A(R2)[31] over 3 months under long-term (25 ± 2 °C/60 ± 5% RH) and accelerated (40 ± 2 °C/75 ± 5% RH) conditions, monitoring drug recovery, viscosity, spreadability, extrudability and assay.

Statistical analysis

All measurements were performed in triplicate. Values are reported as means, with standard deviations given where determined. Model significance in the Box–Behnken design was assessed by analysis of variance within Design-Expert® software. Comparisons between the optimized gel and the marketed product were made using Student's unpaired *t*-test, with $p < 0.05$ considered statistically significant.

RESULTS AND DISCUSSION

Preformulation studies

Miconazole nitrate exhibited poor aqueous and phosphate-buffered saline solubility, consistent with BCS Class II behaviour. The experimentally determined log P was 3.75, close to the reported literature value of 4.07, confirming the drug's lipophilic character and the rationale for nanocrystal-based solubility enhancement. FTIR spectra of the pure drug, poloxamer 407 and their physical mixture showed retention of all characteristic drug bands (C–H aromatic and aliphatic stretching, C≡N and C=N stretching, C=C aromatic stretching and C–Cl stretching) without the appearance of new peaks or the disappearance of existing ones, confirming compatibility. No visible change, colour development, liquefaction or spectral shift was observed for any of the eleven excipients screened (Carbopol 934, oleic acid, glycerin, methyl and propyl paraben, sodium benzoate, HPMC K-

100, triethanolamine, PEG, glycolic acid and PVP) after 30 days at either 25 °C/75% RH or 40 °C/75% RH, indicating that all selected excipients are compatible with miconazole nitrate.

UV method development and validation

Miconazole nitrate showed maximum absorbance at 272 nm in methanol. The calibration curve was linear over 2–10 µg/mL, with the regression equation y = 0.0844x + 0.0032 and a correlation coefficient of 0.9991 (Table 3). Intraday and interday precision (%RSD) ranged from 0.14–0.32% and 0.11–0.93% respectively, both well within the ICH acceptance limit of 2%. Recovery, assessed by the standard addition method at 80%, 100% and 120% of the target concentration, ranged from 99.56 to 100.51% (Table 4), indicating high accuracy. The limit of detection and limit of quantification, calculated from the residual standard deviation of the calibration line and its slope, were 0.35 and 1.07 µg/mL respectively, both below the lowest calibration standard, confirming that the method is sufficiently sensitive for the concentrations encountered in the nanocrystal and gel assays. These results confirm that the developed UV method is simple, precise, accurate and suitable for routine quantitative analysis of miconazole nitrate in nanocrystal and gel formulations.

Table 3: Summary of UV method validation parameters

Parameter	Value
λmax (nm)	272
Linearity range (µg/mL)	2–10
Regression equation	y = 0.0844x + 0.0032
Correlation coefficient (r)	0.9991
Intraday precision (%RSD, n = 3)	0.14–0.32
Interday precision (%RSD, n = 3)	0.11–0.93
System precision (%RSD)	0.42
Method precision (%RSD)	1.3
Accuracy (% recovery, n = 3)	99.56–100.51
LOD (µg/mL)	0.35
LOQ (µg/mL)	1.07

Table 4: Recovery data for the proposed UV method

Amount taken (µg/mL)	Amount added (%)	Mean recovery ± SD (%, n = 3)
6	80	99.56 ± 0.317
6	100	100.51 ± 1.010
6	120	99.67 ± 0.095

Optimization of nanocrystals by Box–Behnken design

Fifteen batches (F1–F15) were prepared per the Box–Behnken design and evaluated for percentage yield and particle size (Table 5). Yield ranged from 62.6 to 86.9% and particle size from 215 to 298 nm. For percentage yield, the model showed a good correlation coefficient ($R^2 = 0.95$); homogenization speed (C) had a statistically significant effect ($p = 0.0003$), while poloxamer 407 concentration (A) and sonication time (B) did not ($p > 0.05$). The positive coefficient for C indicates that yield increased with increasing homogenization speed, consistent with more efficient dispersion and reduced material loss through aggregation. For particle size, the model correlation coefficient was 0.907; both poloxamer 407 concentration ($p = 0.0035$) and sonication time ($p = 0.0172$) significantly affected particle size, whereas homogenization speed did not ($p = 0.09$).

Higher stabilizer concentration and longer sonication both reduced particle size, reflecting more complete surface coverage of newly formed nuclei and more efficient break-up of aggregates. The corresponding response surface plots are presented in Figure 1.

Numerical optimization was performed with the two responses weighted jointly — minimising particle size while maintaining acceptable yield — rather than maximising yield alone. On this basis, the batch containing 1.00% w/v poloxamer 407 with 17.58 min sonication and 2423 rpm homogenization speed returned the highest overall desirability, yielding 72.76% product with a particle size of 256.5 nm (Table 6). This is within the size range reported to favour follicular penetration and reservoir formation in skin, dye-loaded particles of approximately 320 nm having been shown to penetrate hair follicles more deeply and persist longer than the same material in non-particulate form.[32] The predicted and observed responses agreed closely, confirming the validity of the model. Zeta potential was not determined in the present work; since poloxamer 407 stabilizes nanocrystals principally by steric rather than electrostatic means, surface-charge measurement is recommended as a complementary check in future studies.

Table 5: Box–Behnken design layout and observed responses for MNNC batches

Batch	Poloxamer 407 (% w/v)	Sonication time (min)	Homogenization speed (rpm)	Yield (%)	Particle size (nm)
F1	1.00	17.5	3000	76.4	254
F2	1.00	10	5000	82.9	282
F3	1.00	25	1000	62.6	270
F4	0.75	10	3000	74.4	298
F5	1.25	17.5	1000	63.4	253
F6	1.25	10	3000	78.2	232
F7	1.00	17.5	3000	75.8	251
F8	1.00	10	1000	63.8	291
F9	1.00	17.5	3000	75.9	256
F10	1.25	17.5	5000	84.9	246
F11	0.75	17.5	1000	64.4	285
F12	0.75	25	3000	86.9	270

Batch	Poloxamer 407 (% w/v)	Sonication time (min)	Homogenization speed (rpm)	Yield (%)	Particle size (nm)
F13	1.25	25	3000	85.5	215
F14	0.75	17.5	5000	82.5	275
F15	1.00	25	5000	83.7	225

Table 6: Composition and responses of the optimized MNNC batch

Poloxamer 407 (% w/v)	Sonication time (min)	Homogenization speed (rpm)	Yield (%)	Particle size (nm)
1.00	17.58	2423	72.76	256.5

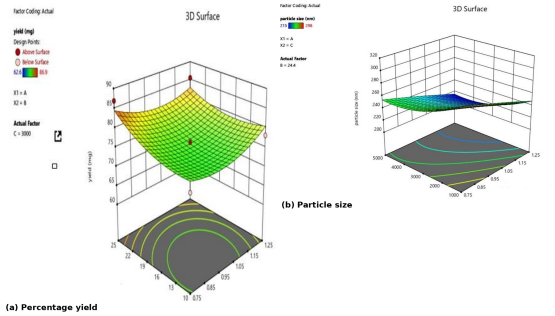

Figure 1: Three-dimensional response surface plots showing the effect of poloxamer 407 concentration, sonication time and homogenization speed on (a) percentage yield and (b) particle size of miconazole nitrate nanocrystals.

Physicochemical characterization of MNNC

FTIR spectra of the optimized MNNC (Figure 2) showed retention of all principal drug bands alongside characteristic poloxamer 407 peaks (O–H stretch at 2956.87 cm^{-1}; asymmetric CH_2 and C–O stretching at 2308.79 and 1651.07 cm^{-1}), indicating successful stabilization without chemical degradation. SEM and optical microscopy (Figure 3) confirmed a narrow size distribution of smooth, irregularly shaped crystalline particles with sharp edges. PXRD of both coarse miconazole nitrate and MNNC (Figure 4) showed characteristic diffraction peaks at $2\theta \approx 15.7°$, 17.6°, 19.2°, 21.1°, 22.6°, 23.8°, 24.0°, 26.0°, 27.2°, 29.1° and 47.1°, confirming that the drug retained its crystalline character after nanoprecipitation. DSC further supported this (Figure 5): the endothermic melting peak of MNNC (149.43 °C) was essentially unchanged from that of the unprocessed drug (150.66 °C), indicating that the crystalline lattice was preserved without significant polymorphic conversion during processing. Retention of crystallinity is desirable for a dermal nanocrystal, since it preserves the physical stability advantage of the crystalline state while the increase in specific surface area supplies the dissolution benefit.

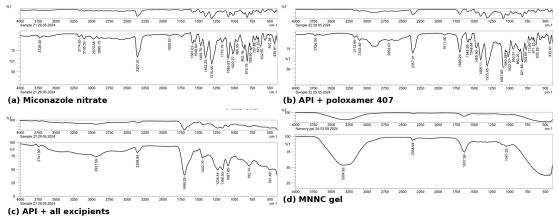

Figure 2: FTIR spectra of (a) pure miconazole nitrate, (b) miconazole nitrate with poloxamer 407, (c) miconazole nitrate with all formulation excipients and (d) the miconazole nitrate nanocrystal gel.

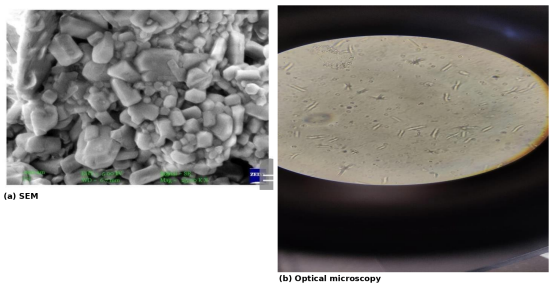

Figure 3: (a) Scanning electron micrograph and (b) optical micrograph of the optimized miconazole nitrate nanocrystals.

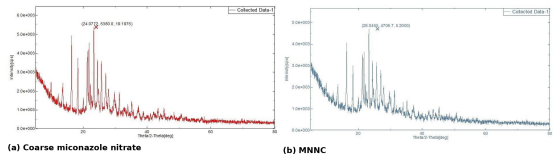

Figure 4: Powder X-ray diffractograms of (a) coarse miconazole nitrate and (b) optimized miconazole nitrate nanocrystals.

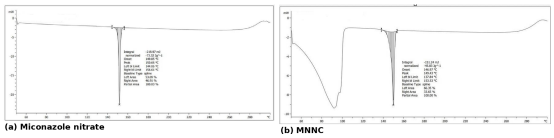

Figure 5: DSC thermograms of (a) pure miconazole nitrate and (b) optimized miconazole nitrate nanocrystals.

Evaluation of MNNC-loaded gel

Five gel batches (H1–H5) with increasing Carbopol 934 concentration were prepared as a screening series and showed a proportional increase in viscosity (892–3480 cP), with a corresponding decrease in spreadability (50.56–16.89 g·cm/s) and assay (89.18–85.79%), reflecting the expected trade-off between polymer concentration, consistency and drug diffusibility (Table 7). All batches maintained a pH of 5.5, within the physiological range of skin. On the combined assessment of viscosity, spreadability, extrudability and *ex vivo* permeability, composition H3 gave the most favourable balance and was selected for scale-up. The optimized batch was then re-prepared at this composition and used for all subsequent definitive evaluation; its properties are reported separately below, and differ slightly from those of the corresponding screening batch, as is expected between preparations.

Table 7: Physicochemical evaluation of the MNNC gel screening series (H1–H5)

Batch	Viscosity (cP)	Spreadability (g·cm/s)	Assay (%)	pH
H1	892	50.56	89.18	5.5
H2	1624	35.42	87.27	5.5
H3	2044	31.11	87.10	5.5
H4	2996	24.23	86.24	5.5
H5	3480	16.89	85.79	5.5

***In vitro* drug release**

Cumulative *in vitro* release from the four gel batches carried forward for dissolution testing is shown in Table 8 and Figure 6. All nanocrystal-loaded batches released substantially more drug at every time point than the marketed reference gel, with batch H3 reaching 86.5% at 7 h compared with 53.9% for the marketed product ($p < 0.05$). Release from H3 exceeded 60% within 4 h, whereas the marketed gel released only 13.7% over the same period. This enhancement is attributable to the increased effective surface area and saturation solubility conferred by particle size reduction to the nanoscale, consistent with the Noyes–Whitney relationship,[33] and is further assisted by the lower viscosity of the formulated gel relative to the marketed product.

Table 8: Cumulative *in vitro* drug release (% CDR) from the MNNC gel screening series versus the marketed gel

Time (h)	H1	H2	H3	H4	Marketed gel
1	7.4	10.5	19.8	10.0	4.5
2	11.4	19.6	27.2	16.6	6.0
3	19.6	32.0	38.4	26.3	9.2
4	39.6	52.4	60.4	50.7	13.7
5	54.0	68.8	76.5	64.7	22.7
6	65.0	76.2	81.2	72.4	33.2
7	73.9	82.4	86.5	81.7	53.9

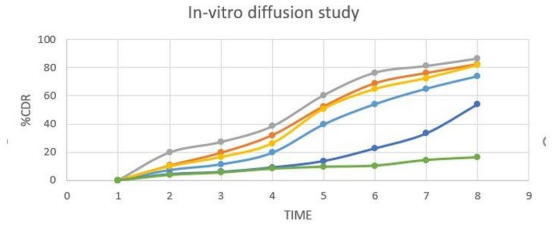

Figure 6: Cumulative *in vitro* drug release profiles of MNNC gel batches H1–H4 and the marketed miconazole gel in pH 5.5 acetate buffer at 37 ± 0.5 °C. Each value is the mean of three determinations.

***Ex vivo* permeation and skin retention**

Ex vivo permeation of the optimized gel through excised goat skin reached 48.03% cumulative permeation over 8 h (Table 9, Figure 7). Layer-wise dissection of the skin at the end of the study showed that, of the drug recovered from the tissue, 77.16% was retained in the epidermis, 15.42% in the stratum corneum and 7.42% in the dermis (Table 10). This distribution is consistent with a reservoir-type deposition pattern favourable for treating epidermally localized fungal infection, and mirrors the behaviour reported for other dermal azole

nanocrystal systems, in which the nanocrystalline form raised total skin retention to 62.17% against 41.87% for a coarse drug suspension.[16,19] The optimized gel showed markedly higher cumulative release than the marketed product at every time point (Table 8), despite the marketed gel exhibiting substantially higher viscosity and lower spreadability (Table 11) — differences consistent with the improved dissolution and diffusibility conferred by the nanocrystalline drug form and with the lipid-disordering action of glycolic acid in the vehicle.

Table 9: *Ex vivo* permeation of the optimized gel through excised goat skin

Time (h)	0	1	2	3	4	5	6	7	8
Cumulative permeation (%)	0	13.50	20.85	23.79	28.96	34.50	35.49	45.48	48.03

Table 10: Distribution of drug retained within the skin layers after 8 h (optimized gel)

Skin layer	Proportion of skin-retained drug (%)
Stratum corneum	15.42
Epidermis	77.16
Dermis	7.42
Total	**100.00**

Table 11: Optimized MNNC gel compared with the marketed miconazole gel

Formulation	Viscosity (cP)	Spreadability (g·cm/s)	Extrudability (%)	pH	Assay (%)
Optimized MNNC gel	2112	34.41	88.19	5.5	94.2
Marketed gel	10984	13.11	89.09	5.5	97.7

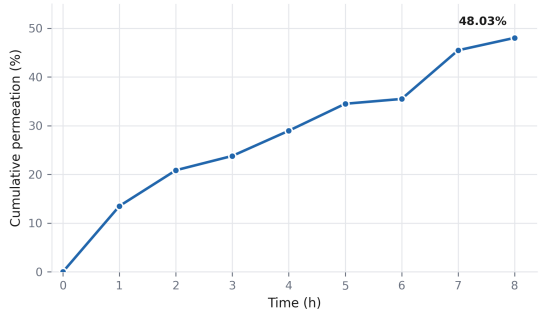

Figure 7: *Ex vivo* cumulative permeation profile of the optimized MNNC gel through excised goat skin over 8 hours (data as Table 9).

***In vitro* antifungal activity**

The MNNC-incorporated gel produced a significantly larger zone of inhibition against *C. albicans* (25 ± 0.15 mm) than the marketed miconazole sample (15 ± 0.15 mm) at equivalent drug loading ($p < 0.05$; Figure 8). This enhanced antifungal potency is attributed to two complementary effects: faster dissolution and a greater effective concentration of miconazole nitrate at the site of action owing to the nanocrystalline form, and the keratolytic and lipid-disordering contribution of glycolic acid, which increases access of the azole to the fungal cell. These results suggest that comparable or superior antifungal efficacy could be achieved with the formulated gel at a reduced dose relative to the conventional marketed product.

Two limitations of this assay should be acknowledged. Diffusion plates were prepared on nutrient agar rather than Sabouraud dextrose agar, which is the medium conventionally recommended for *Candida*; because both formulations were tested

on the same medium in the same run, the relative difference between them is internally controlled, but absolute zone diameters are not directly comparable with values obtained on Sabouraud dextrose agar. In addition, the individual contribution of glycolic acid was not isolated in the present study; a glycolic acid-free nanocrystal gel control is required to apportion the observed enhancement between the nanocrystalline state and the co-agent. Determination of minimum inhibitory concentrations on Sabouraud dextrose agar, together with that control arm, forms the basis of ongoing work.

Figure 8: Representative agar well diffusion plate against *Candida albicans* (MTCC 183) showing the zone of inhibition produced by the MNNC-loaded gel (Test) alongside the control well.

Stability studies

Short-term storage indicated that nanocrystal size was largely stable at 2 °C, whereas storage at room temperature and, more markedly, at 40 °C led to an increase in particle size, consistent with Ostwald ripening and reduced efficiency of steric stabilization at elevated temperature. Over 3 months of ICH-condition storage, drug recovery in the nanocrystal fraction declined modestly from 68.90% to 66.74% under long-term conditions and to 64.97% under accelerated conditions, with corresponding small reductions in dissolution and assay (Table 12). The optimized gel likewise showed only minor changes in viscosity, spreadability, extrudability and assay under both conditions (Table 13), with no phase separation, discoloration or loss of homogeneity, confirming that the MNNC-loaded gel is physically and chemically stable over the period tested.

Table 12: Stability of the miconazole nitrate nanocrystals over 3 months. LT = long-term storage (25 ± 2 °C / 60 ± 5% RH); Acc. = accelerated storage (40 ± 2 °C / 75 ± 5% RH); dissolution measured in pH 5.5 acetate buffer

Parameter	1 mo LT	1 mo Acc.	2 mo LT	2 mo Acc.	3 mo LT	3 mo Acc.
Drug recovery in nanocrystal fraction (%)	68.90	67.92	68.24	67.22	66.74	64.97
Dissolution at 8 h (%)	90.28	85.45	91.23	82.26	88.72	87.48
Assay (%)	92.25	92.16	90.20	88.26	89.26	87.23

Table 13: Stability of the optimized MNNC gel over 3 months. LT = long-term storage (25 ± 2 °C / 60 ± 5% RH); Acc. = accelerated storage (40 ± 2 °C / 75 ± 5% RH)

Parameter	1 mo LT	1 mo Acc.	2 mo LT	2 mo Acc.	3 mo LT	3 mo Acc.
Viscosity (cP)	2104	2100	2018	2107	2005	1990

Parameter	1 mo LT	1 mo Acc.	2 mo LT	2 mo Acc.	3 mo LT	3 mo Acc.
Spreadability (g·cm/s)	35.61	37.26	38.92	42.44	41.88	48.26
Extrudability (%)	88.10	90.26	90.28	93.49	94.88	92.72
Assay (%)	94.21	94.45	92.50	90.44	90.17	88.63

CONCLUSION

Miconazole nitrate nanocrystals were successfully prepared by nanoprecipitation and optimized using a Box–Behnken statistical design, yielding particles of 256.5 nm at 72.76% yield with poloxamer 407 as stabilizer. A simple, precise and accurate UV spectrophotometric method (linear over 2–10 µg/mL, r = 0.9991) enabled reliable quantification throughout formulation development. Incorporation of the optimized nanocrystals into a Carbopol 934 gel with glycolic acid produced a formulation with acceptable pH, viscosity, spreadability and extrudability, and substantially enhanced *in vitro* drug release compared with a marketed miconazole gel. *Ex vivo* study through excised goat skin gave appreciable permeation over 8 hours with the recovered drug preferentially retained in the epidermis, a distribution favourable for treating epidermally localized infection. The formulated gel exhibited greater antifungal activity against *C. albicans* than the marketed product under the conditions tested, and remained stable over 3 months of ICH-condition storage. Collectively, these findings indicate that combining nanocrystal technology with a keratolytic penetration enhancer such as glycolic acid is a viable strategy to overcome the solubility-limited topical delivery of miconazole nitrate. Isolation of the specific contribution of glycolic acid using a co-agent-free control, confirmation of antifungal activity on Sabouraud dextrose agar with minimum inhibitory concentrations, and *in vivo* efficacy and long-term stability studies form the basis of continuing work.

ACKNOWLEDGEMENTS

The authors thank the Department of Pharmaceutics, H. K. College of Pharmacy, Oshiwara, Mumbai, for providing the facilities necessary to carry out this work, and Maharshee Laboratories Pvt. Ltd. for the gift sample of miconazole nitrate.

CONFLICT OF INTEREST

The authors declare no conflict of interest.

REFERENCES

1. Amidon GL, Lennernäs H, Shah VP, Crison JR. A Theoretical Basis for a Biopharmaceutic Drug Classification: The Correlation of In Vitro Drug Product Dissolution and In Vivo Bioavailability. Pharmaceutical Research. 1995;12(3):413-420. DOI: 10.1023/A:1016212804288
2. Jarvis M, Krishnan V, Mitragotri S. Nanocrystals: A Perspective on Translational Research and Clinical Studies. Bioengineering & Translational Medicine. 2019;4(1):5-16. DOI: 10.1002/btm2.10122
3. Li J, Wang Z, Zhang H, Gao J, Zheng A. Progress in the Development of Stabilization Strategies for Nanocrystal Preparations. Drug Delivery. 2021;28(1):19-36. DOI: 10.1080/10717544.2020.1856224
4. Tapfumaneyi P, Imran M, Mohammed Y, Roberts MS. Recent Advances and Future Prospective of Topical and Transdermal Delivery Systems. Frontiers in Drug Delivery. 2022;2:957732. DOI: 10.3389/fddev.2022.957732
5. Ghasemiyeh P, Mohammadi-Samani S. Potential of Nanoparticles as Permeation Enhancers and Targeted Delivery Options for Skin: Advantages and Disadvantages. Drug Design, Development and Therapy. 2020;14:3271-3289. DOI: 10.2147/DDDT.S264648
6. Raszewska-Famielec M, Flieger J. Nanoparticles for Topical Application in the Treatment of Skin Dysfunctions – An Overview of Dermo-Cosmetic and Dermatological Products. International Journal of Molecular Sciences. 2022;23(24):15980. DOI: 10.3390/ijms232415980
7. Sousa F, Ferreira D, Reis S, Costa P. Current Insights on Antifungal Therapy: Novel Nanotechnology Approaches for Drug Delivery Systems and New Drugs from Natural Sources. Pharmaceuticals. 2020;13(9):248. DOI: 10.3390/ph13090248
8. Hay RJ, Ashbee HR. Fungal Infections. In: Griffiths C, Barker J, Bleiker T, Chalmers R, Creamer D, editors. Rook's Textbook of

Dermatology. 9th ed. Chichester: Wiley-Blackwell; 2016. p. 1-110. DOI: 10.1002/9781118441213.rtd0033
9. Nett JE, Andes DR. Antifungal Agents: Spectrum of Activity, Pharmacology, and Clinical Indications. Infectious Disease Clinics of North America. 2016;30(1):51-83. DOI: 10.1016/j.idc.2015.10.012
10. Bhalekar MR, Pokharkar V, Madgulkar A, Patil N, Patil N. Preparation and Evaluation of Miconazole Nitrate-Loaded Solid Lipid Nanoparticles for Topical Delivery. AAPS PharmSciTech. 2009;10(1):289-296. DOI: 10.1208/s12249-009-9199-0
11. Al-Maghrabi PM, Khafagy ES, Ghorab MM, Gad S. Influence of Formulation Variables on Miconazole Nitrate-Loaded Lipid Based Nanocarrier for Topical Delivery. Colloids and Surfaces B: Biointerfaces. 2020;193:111046. DOI: 10.1016/j.colsurfb.2020.111046
12. Tejada G, Barrera MG, García P, Sortino M, Lamas MC, Lassalle V, Alvarez V, Leonardi D. Nanoparticulated Systems Based on Natural Polymers Loaded with Miconazole Nitrate and Lidocaine for the Treatment of Topical Candidiasis. AAPS PharmSciTech. 2020;21(7):278. DOI: 10.1208/s12249-020-01826-6
13. Rasool M, Mazhar D, Afzal I, Zeb A, Khan S, Ali H. In Vitro and In Vivo Characterization of Miconazole Nitrate Loaded Transethosomes for the Treatment of Cutaneous Candidiasis. International Journal of Pharmaceutics. 2023;647:123563. DOI: 10.1016/j.ijpharm.2023.123563
14. Cerdeira AM, Mazzotti M, Gander B. Miconazole Nanosuspensions: Influence of Formulation Variables on Particle Size Reduction and Physical Stability. International Journal of Pharmaceutics. 2010;396(1-2):210-218. DOI: 10.1016/j.ijpharm.2010.06.020
15. Cerdeira AM, Mazzotti M, Gander B. Formulation and Drying of Miconazole and Itraconazole Nanosuspensions. International Journal of Pharmaceutics. 2013;443(1-2):209-220. DOI: 10.1016/j.ijpharm.2012.11.044
16. Pyo SM, Hespeler D, Keck CM, Müller RH. Dermal Miconazole Nitrate Nanocrystals – Formulation Development, Increased Antifungal Efficacy and Skin Penetration. International Journal of Pharmaceutics. 2017;531(1):350-359. DOI: 10.1016/j.ijpharm.2017.08.108
17. Kumar P, Singh AK, Almalki WH, Alruwaili NK, Alzahrani A, Alhamyani A, Altamimi ASA, Singh AK, Sahoo A, Haneef J, Singh T, Rahman M. Development, Characterization, In Vitro, Ex Vivo, and Stability Evaluation of a Miconazole Nitrate Nanocrystal-Loaded Hydrogel for Topical Application. Current Medicinal Chemistry. 2026;33(4):835-859. DOI: 10.2174/0109298673339390250605054706
18. Abdel-Rashid RS, Helal DA, Alaa-Eldin AA, Abdel-Monem R. Polymeric versus Lipid Nanocapsules for Miconazole Nitrate Enhanced Topical Delivery: In Vitro and Ex Vivo Evaluation. Drug Delivery. 2022;29(1):294-304. DOI: 10.1080/10717544.2022.2026535
19. Kumar M, Shanthi N, Mahato AK, Soni S, Rajnikanth PS. Preparation of Luliconazole Nanocrystals Loaded Hydrogel for Improvement of Dissolution and Antifungal Activity. Heliyon. 2019;5(5):e01688. DOI: 10.1016/j.heliyon.2019.e01688
20. Doshi A, Prabhakar B, Wairkar S. Prolonged Retention of Luliconazole Nanofibers for Topical Mycotic Condition: Development, In Vitro Characterization and Antifungal Activity against Candida albicans. Journal of Materials Science: Materials in Medicine. 2024;35(1):46. DOI: 10.1007/s10856-024-06815-w
21. El-Housiny S, Shams Eldeen MA, El-Attar YA, Salem HA, Attia D, Bendas ER, El-Nabarawi MA. Fluconazole-Loaded Solid Lipid Nanoparticles Topical Gel for Treatment of Pityriasis Versicolor: Formulation and Clinical Study. Drug Delivery. 2018;25(1):78-90. DOI: 10.1080/10717544.2017.1413444
22. Peng LH, Wei W, Shan YH, Chong YS, Yu L, Gao JQ. Sustained Release of Piroxicam from Solid Lipid Nanoparticle as an Effective Anti-Inflammatory Therapeutics In Vivo. Drug Development and Industrial Pharmacy. 2017;43(1):55-66. DOI: 10.1080/03639045.2016.1220563
23. Dampa E. The Effectiveness of Topical Keratolytics (Alpha Hydroxy Acids/Beta Hydroxy Acids/Urea) in Treating Keratosis Pilaris: A Review of the Literature. Cureus. 2025;17(12):e100507. DOI: 10.7759/cureus.100507
24. International Council for Harmonisation. ICH Q2(R1): Validation of Analytical Procedures – Text and Methodology. Geneva: ICH; 2005.
25. Martínez Rivas CJ, Tarhini M, Badri W, Miladi K, Greige-Gerges H, Nazari QA, Galindo Rodríguez SA, Álvarez Román R, Fessi H, Elaissari A. Nanoprecipitation

Process: From Encapsulation to Drug Delivery. International Journal of Pharmaceutics. 2017;532(1):66-81. DOI: 10.1016/j.ijpharm.2017.08.064

26. Ferreira SLC, Bruns RE, Ferreira HS, Matos GD, David JM, Brandão GC, da Silva EGP, Portugal LA, dos Reis PS, Souza AS, dos Santos WNL. Box-Behnken Design: An Alternative for the Optimization of Analytical Methods. Analytica Chimica Acta. 2007;597(2):179-186. DOI: 10.1016/j.aca.2007.07.011
27. Islam MT, Rodríguez-Hornedo N, Ciotti S, Ackermann C. Rheological Characterization of Topical Carbomer Gels Neutralized to Different pH. Pharmaceutical Research. 2004;21(7):1192-1199. DOI: 10.1023/B:PHAM.0000033006.11619.07
28. Kansagra H, Mallick S. Microemulsion-Based Antifungal Gel of Luliconazole for Dermatophyte Infections: Formulation, Characterization and Efficacy Studies. Journal of Pharmaceutical Investigation. 2016;46(1):21-28. DOI: 10.1007/s40005-015-0209-9
29. Organisation for Economic Co-operation and Development. OECD Guideline for the Testing of Chemicals No. 428: Skin Absorption – In Vitro Method. Paris: OECD Publishing; 2004.
30. Ahmad N, Ahmad R, Mohammed Buheazaha T, Salman AlHomoud H, Al-Nasif HA, Sarafroz M. A Comparative Ex Vivo Permeation Evaluation of a Novel 5-Fluorocuracil Nanoemulsion-Gel by Topically Applied in the Different Excised Rat, Goat, and Cow Skin. Saudi Journal of Biological Sciences. 2020;27(4):1024-1040. DOI: 10.1016/j.sjbs.2020.02.014
31. International Council for Harmonisation. ICH Q1A(R2): Stability Testing of New Drug Substances and Products. Geneva: ICH; 2003.
32. Lademann J, Richter H, Teichmann A, Otberg N, Blume-Peytavi U, Luengo J, Weiss B, Schaefer UF, Lehr CM, Wepf R, Sterry W. Nanoparticles – An Efficient Carrier for Drug Delivery into the Hair Follicles. European Journal of Pharmaceutics and Biopharmaceutics. 2007;66(2):159-164. DOI: 10.1016/j.ejpb.2006.10.019
33. Noyes AA, Whitney WR. The Rate of Solution of Solid Substances in Their Own Solutions. Journal of the American Chemical Society. 1897;19(12):930-934. DOI: 10.1021/ja02086a003